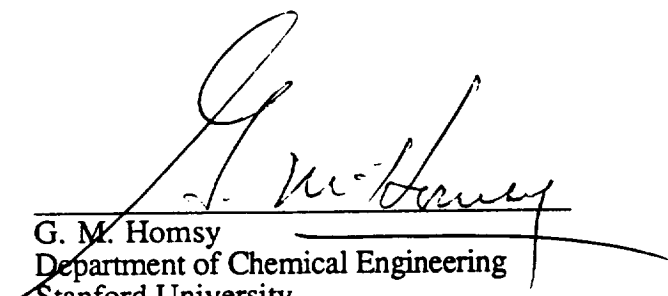


Final Report


Final
NASA-CR
OCIT.
10/10/77

"Moisture Content and Migration Dynamics in Unsaturated Porous Media"

NASA - Ames Grant NCC2-5104



G. M. Homsy
Department of Chemical Engineering
Stanford University
Stanford CA 94305-5025



Mark Kliss
NASA Ames Research Center
Mail Stop 223-9, PO Box 1000
Moffett Field, CA 94035-1000

Summary

This is the final report on our one year grant for the study of "Moisture Content and Migration Dynamics in Unsaturated Porous Media". We proposed fundamental studies of fluid mechanics and transport in partially saturated soils. Two studies were envisioned. In the first, an undergraduate student would be involved in the solution of transient diffusion problems in support of the development of probes for the in-situ measurement of moisture content. In the second, numerical and analytical methods were to be used to study the fundamental problem of meniscus and saturation front propagation in geometric models of porous media.

The first project involved Mr. James MacDonald, an undergraduate in Chemical Engineering at Stanford, working closely with Dr. Boris Yendler, an NRC Fellow at NASA Ames. Dr. Yendler had responsibility for the day to day progress of Mr. MacDonald: Prof. Homsy reviewed the work on a periodic basis and made some technical suggestions regarding the series expansion and inversion of Laplace transforms. Mr. MacDonald and Dr. Yendler have co-authored a paper, a copy of which is appended.

The second project began with the engagement of Mr. Ahmed Farooq, an advanced PhD student in Mechanical Engineering at Stanford. Following some initial discussions between Mr. Farooq, Dr. Yendler and Prof. Homsy, Mr. Farooq conducted a short assessment of the applicability of standard 'soil science' models to treat the problem of the propagation of saturation fronts in porous media. Mr. Farooq's progress was not entirely satisfactory, and it was decided that he should leave the project. His short report is also appended. Following this, Prof. Homsy took the opportunity to acquire a flexible finite element program for the solution of meniscus propagation in pore spaces. This opportunity was afforded by the sabbatical visit of Prof. Bamin Khomami from Washington University, St. Louis. The program has been acquired and another of Prof. Homsy's PhD students, Ms. Jean Ro, has familiarized herself with the program and has completed some benchmark runs. A short description of the program and its capabilities is also attached. Although the budgeted funds have been expended, Ms. Ro is continuing to work on the problem of meniscus propagation through geometrically complex pore space, and all publications based on her work will carry an appropriate acknowledgement to the NASA grant that allowed the acquisition of the finite element program.

James MacDonald

NASA Summary

Project Definition and Objectives

This work was undertaken in response to a problem encountered while determining thermal conductivity characteristics of partially saturated soils. Ongoing research utilized a cylindrical "thermal probe" containing a heat source and a transducer in order to measure thermal dissipation within a homogenous partially saturated soil that was packed via protocol (please see attachment "Moisture Measurements" for reasoning of probe selection). An IBM computer was then used to interpret the transducer pulses resulting in profiles of temperature versus time. These profiles were then utilized to back-calculate the thermal conductivity of the medium. The problem was that the resulting profiles differed depending on the spatial placement of the sensors. For example, if a sensor was placed in the medium a temperature profile would be obtained, but if the same sensor was placed in a different area of the homogeneous medium, a different profile was obtained.

The multiple curves show a difference both in magnitude and slope during short time, but the long time data only shows a magnitude offset which is presumed to be due to the offset introduced in the short time regime. This observed offset is hypothesized to be a result of variations in the contact resistivity at the sensor's surface. The variance occurred due to difference in soil packing around the sensor upon each insertion. This work will attempt to minimize or eliminate the variance in the contact resistivity effect in order to collapse the numerous experimental curves into one accurate curve which will allow the calculation of the medium's thermal conductivity.

Approach To Solution

Prior to this work, the first attempt to isolate the contact resistivity resulted in applying the cylindrical "thermal probe" equations derived by Blackwell¹ to the data. This included both the original equations and the long time probe and short time medium equations he combined in an attempt to account for the conductivity of the probe. Without knowing the heat transfer coefficient, the variable that describes the contact resistivity, or the thermal conductivity of the medium, the theoretical equations for short and long time were solved for both terms. This same procedure was carried out for multiple runs within the same medium but failed to reproduce a consistent thermal conductivity.

This failure brought into question the validity of one of the primary assumptions of Blackwell's original equations - that the composite of the sensor itself provides no resistance to the heat. Secondly, the applicability of his "combined" equations that account for the contact resistivity are questioned in this scenario. In order to gain better information about the contact resistivity, this work rederives Blackwell's short time equation and includes the heat propagation into the sensor. This equation attempts to provide more accurate information about the time regime where contact resistivity is dominant in order to eliminate the observed variance.

Summary of Results

The preliminary resulting short time equation with first term approximations results in the following equation in the Laplace domain:

$$T_p = \frac{\phi}{T_1} \frac{\left[1 + \frac{Bio}{T_2^{1/2}} s^{-1/2} \right]}{\left[1 + \frac{Bio}{T_2^{1/2}} s^{-1/2} + \frac{2Bio}{T_1 s} s^{-1} \right]} \quad (1)$$

¹Blackwell, J.H. *A Transient-Flow Method for Determination of Thermal Constants of Insulating Materials in Bulk.* *Journal of Applied Physics.* Vol. 25, Number 2, February, 1954. p. 137-144.

where

$$\phi = \frac{2Q'R}{\lambda_1 T_c} \quad \text{Bio} = \frac{HR}{\lambda_2} \quad \varepsilon = \frac{\lambda_1}{\lambda_2} \quad T_1 = \frac{D_1}{R^2} \quad T_2 = \frac{D_2}{R^2} \quad (2)$$

and Q' is the power supplied per unit area of the sensor, R is the radius of the sensor, λ_1 is the thermal conductivity of the sensor, T_c is the characteristic temperature, H is the heat transfer coefficient, λ_2 is the thermal conductivity of the medium, D_1 is the diffusivity of the probe and D_2 is the diffusivity of the medium. Equation (1) represents a more accurate approximation than Blackwell's equation. If the third term of the denominator in Equation (1) is dropped, the denominator is approximated with the a Taylor expansion, and finally the inverse Laplace transform is taken the equation reduces to the exact equation Blackwell presented:

$$T_p = \phi \left[\frac{t}{T_1} + \frac{\text{Bio}}{\varepsilon} \left(\frac{t}{T_1} \right)^2 + \frac{16\text{Bio}^2}{15\sqrt{\pi\varepsilon}} \left(\frac{t}{T_1} \right)^2 \left(\frac{t}{T_2} \right)^{1/2} + O(t^3) \right] \quad (3)$$

The next step was to take the second term approximation which resulted in the following equation which is still in the Laplace transform domain:

$$T_p = \frac{2\phi}{T_1} s^{-2} \left[\frac{1 - \frac{\text{Bio}}{2T_1 T_2} s^{-2} + \left(\frac{4\text{Bio}}{T_1 T_2^{1/2}} + \frac{3}{2T_1 T_2^{1/2}} \right) s^{-3/2} + \left(\frac{4}{T_1} - \frac{\text{Bio}}{8T_2} \right) s^{-1} + \left(\frac{3}{8T_2^{1/2}} + \frac{\text{Bio}}{T_2^{1/2}} \right) s^{-1/2}}{1 - \left(\frac{2\text{Bio}}{T_1 T_2^{1/2}} \right) s^{-5/2} + \left(\frac{16\text{Bio}}{T_1^2} - \frac{\text{Bio}}{T_1 T_2} \right) s^{-2} + \left(\frac{8\text{Bio}}{T_1 T_2^{1/2}} - \frac{\text{Bio}}{2T_1 T_2^{1/2}} + \frac{3}{T_1 T_2^{1/2}} \right) s^{-3/2} + \left(\frac{8}{T_1} + \frac{4\text{Bio}}{T_1 \varepsilon} - \frac{\text{Bio}}{8T_2} \right) s^{-1} + \left(\frac{3}{8T_2^{1/2}} + \frac{\text{Bio}}{T_2^{1/2}} \right) s^{-1/2}} \right] \quad (4)$$

where s is the transform variable. This equation is currently being reviewed and further results should be available by January 1, 1996. The initial division of this solution using a Taylor expansion produces an poor polynomial approximation. This invalid approximation does have the same time dependence as Blackwell's solution but the expected deviation occurs in the coefficients which incorporate the thermal conductivity of the probe. Another approximation technique is currently being sought.

Preliminary results show inclusion of the probe resistance alters the short time temperature profile solution presented by Blackwell. Although the time dependence remains the same, the coefficients show significant deviation. This deviation provides promise that a more accurate solution will be obtained and ultimately lead to an isolation of the variance provided by the contact resistivity.

Overall Summary

Ongoing research investigating thermal conductivities of partially saturated soils has led to the need for an improved mathematical model of cylindrical "thermal sensors". Measurement trials have led to the obtainment of various temperature profiles for the same homogeneous medium. This inconsistency in data acquisition has been hypothesized to be due to a variance in contact resistivity at the probe's surface because of varied soil packing around the probe upon insertion. Previously, Blackwell's short and long time temperature profile equations were utilized in an attempt to iterate for the values of both the thermal conductivity and the heat transfer coefficient, the variable describing the contact resistivity. This iteration failed to provide a reproducible thermal conductivity. This work has improved upon a basic assumption of Blackwell's work - that the probe itself provides no resistance to heat transfer. Incorporating the heat transfer into the probe within the model has led to a deviation from Blackwell's work. The first term approximations are identical but the preliminary second term approximations show the same time dependence with different coefficients. The continuing work should provide a more accurate mathematical model which will allow the isolation of contact resistivity's influence and thus allow a consistent and accurate thermal conductivity to be evaluated.

MOISTURE MEASUREMENTS

The most important indication of water state (especially in microgravity) would be the direct measurement of the free energy status of the water in the system. Given the free energy distribution of the water in a root module, movement and availability to plants could be easily calculated. Matrix potential (energy level) can be measured directly by a tensiometer, but these sensors are typically bulky, require significant care, and have not been proven in space yet (Ref. 4). Since moisture content and matrix potential are functions of one another, matrix potential is usually inferred from water content measurements.

Current state-of-the-art methods for determining sub-strate water content include neutron attenuation, gamma ray attenuation, gypsum blocks, Time Domain Reflectometry (TDR), and heat pulse. The first two methods, neutron attenuation and gamma ray attenuation, pose a radiation hazard and tend to be bulky devices. Gypsum blocks have been available for terrestrial measurements for years, but they require high frequencies and are not overly sensitive. The TDR method has become popular because it is flexible, accurate, and measures rapidly. Traditional TDR does require complex circuitry, however, and uses high radio frequencies (2 - 3 GHz) which would cause concern aboard a spacecraft. Smaller, more portable, capacitance-based TDR units are being developed which may increase their potential for use in space. Whereas, the gypsum block method relates electrical to water content, the heat pulse method uses changes in thermal conductivity to infer moisture level (Ref. 4).

The heat pulse-type sensor was widely used for moisture level measurements in substrates during plant experiments (Refs. 1, 2, 5, and 6). Based on the experience gained from these experiments and measurements from prototype sensors, a heat pulse-type sensor was developed for the GEMS unit. A TDR-type system was also investigated, but it was determined that the cost and long qualification time required for acceptance of this type sensor made it unacceptable. Limitation in power requirements, electromagnetic emissions, and automation aboard a spacecraft place stringent constraints on available measurement techniques. While the heat pulse-type sensor has the advantages of low average power consumption and simplistic design, it also has the disadvantage of depending on heat conductivity for measurement instead of a direct measurement of moisture content or matrix potential of the media. Other factors like particle diameter of a substrate and resistance to a heat flow between a moisture sensor and surrounding media, referred to as contact resistance, can affect a heat pulse measurement of moisture level within a substrate.

Recently, heat pulse sensors have been developed with a solid porous ceramic coating (Ref. 6). These sensors correlate the water content of the ceramic coating with the sensor temperature rise. Because the temperature rise of the sensor is dependent on the water content of the ceramic coating, other factors like particle diameter cause less impact on the sensor readings. When placed in a soil, the water potential of the ceramic comes into equilibrium with the free energy level of the water in the soil. Hence, the sensor can be calibrated directly as a function of the water potential of the surrounding media. Because the probe is in constant and rigid contact with the ceramic, the problems associated with the use of bare probes in varying sized media (contact resistance) is eliminated.

Although the ceramic surrounding the probe has a known temperature rise to water potential (water content) relationship, the use of the sensor is dependent on the ability of the ceramic to exchange water with the matrix to be measured. The ceramic used in these applications is usually rather fine grained to match the structures of agricultural soils. It has since been discovered that the system does not work effectively with the large grained substrates used in space. The probe must stay in equilibrium with the substrate. This is possible only if the hydraulic conductivity of the small grained ceramic has a similar unsaturated hydraulic conductivity as the substrate. The substrate used in Svet system does not meet this requirement. Selecting smaller substrates will eventually allow the direct measurement of matrix potential using this sensor.

REFERENCES

1. Ivanova, T. N. and I. W. Dandolov, "Dynamics of the Controlled Environment Conditions in Svet Greenhouse in Flight," *Comptes rendus del'Academie bulgare Science*, Tome 45, No. 3, pp. 33-35, 1992.

2. Ivanova, T. N., Y. A. Berkovich, A. L. Mashinsky, and G. I. Meleshko, "The First Space Vegetables to be Grown in the Svet Greenhouse by Means of Controlled Environmental Conditions," *Microgravity Q.*, Vol.2, No. 2, p. 109, 1992.
3. Bingham, G. E., F. B. Salisbury, W. F. Campbell, J. G. Carman, D. L. Bubenheim, B. Yendler, V. N. Sytchev, Y. A. Berkovich, M. A. Levinshkin, and I. G. Podolsky, "The SpaceLab/Mir-1 Greenhouse 2 Experiment," 1995 (in press).
4. Gardner, W. H. "Water Content," A. Klute (Ed.), "Methods of Soil Analysis," Part I. Monograph 9, *American Society of Agronomy*, Madison, WI, pp 493-544, 1986.
5. Foth, W. P. and H. Löser, "Design and Development of the Life Support Subsystem of a Laboratory Model of the Botany Facility," SAE Technical Paper No. 871519, 17th Intersociety Conference on Environmental Systems, Seattle, WA, July 13-15, 1987.
6. Phene, C. J., G. J. Hoffinan, and S. L. Rawlins, "Measuring Soil Potential in situ by Sensing Heat Distribution with a Porous Body: I. Theory and Sensor Construction," *Soil Sci. Amer. Proc.*, Vol. 35, pp. 27-33, 1973.

Propagation of menisci into pore space:
Simulation by finite elements

Jean Ro

The finite element method has been successfully applied to non-linear fluid mechanics problems. Finite element algorithms make use of the weak forms of the basic equations of motion and continuity equations. The solution is obtained as an approximation to the unknown functions using trial functions defined over individual elements. The main advantage of the finite element method is that the elements do not have to be of uniform size or shape. Therefore, irregular domains require no special handling - a particular advantage in dealing with free boundary problems such as ours. In addition, more efficient computation can be achieved by using smaller elements in regions of rapid variations of the dependent variables, or by raising the degree of the polynomials which are used as trial functions.

For application to free boundary problems, or when the fluid is viscoelastic, it is useful to work with stress as a dependent variable. The weak form of the equation of motion contains stresses which are implicit functions of the velocity field, since in the general non-Newtonian case, stress components cannot be given as algebraic functions of the velocity components and their derivatives. Prof. Khomami's finite element code treats the deviatoric stress tensor as the sum of the polymeric (T_p) and Newtonian (T_s) solvent stress tensor, with the two being related to appropriate flow variables by a given constitutive relations. In the mixed method, the extra stresses are treated as unknowns, and are assumed as linear combinations of trial functions just as the velocity and the pressure are treated. Newtonian flow problems can be treated simply by setting the polymeric stress components to zero and using the Newtonian relationship between stress and rate of strain. For viscoelastic flow problems, this mixed method is combined with the elastic-viscous split stress technique (EVSS) in which the deviatoric stress is divided into elastic and viscous portions, with the viscous part including the Newtonian contributions from both the solvent part of the stress and the polymer part. The advantage of adopting the EVSS method is that convergent solutions can be obtained regardless of the value of the ratio between the solvent viscosity and the viscosity of the solution since equations are rewritten in an explicitly elliptic way. The overall strategy in the code is to solve the continuity and momentum equations, which contain an elliptic operator, by Galerkin's method, and to compute stresses by Streamline Upwinding Petrov-Galerkin method (SUPG) which is suitable for hyperbolic equations. Quadrilateral elements are allowed. Biquadratic shape functions are used for stresses and velocity, and bilinear shape functions are used for the rate of strains and pressure. There are total of ten variables per element.

The finite element method is well suited for our free surface problem with the irregular domain. In our iterative formulation, the finite element solver mentioned above is used to solve for the two dimensional flow with the kinematic and tangential stress boundary conditions imposed on the assumed free boundary which is unknown a-priori. Then the computed pressure and normal stresses, together with the normal stress balance, are used to correct the free boundary location. That is accomplished by solving the differential equation resulting from the normal stress balance equation using the finite element method with one dimensional free surface as our domain. The normal stress condition depends on the curvature of the free surface, whereas the kinematic and tangential stress boundary conditions depend only on surface orientation. Therefore, the normal stress scheme mentioned above is more likely to converge than other possible schemes.

We are currently in the process of validation of this procedure by solving the problem of meniscus propagation between parallel plates at finite capillary number. This will be followed by a study of meniscus propagation between spatially varying walls more appropriate to geometric models of porous media.

Flow of Water through a Bed of Packed Spheres

A. Farooq

Dept. of Mechanical Engineering, Stanford University, Stanford, CA 94305.

1 Introduction

Some recent experiments (Yendler et al. 1993) have investigated the propagation of water through a bed of packed spheres. The motivation is to investigate the propagation of water in micro-gravity environments with the objective of growing plants in space. Their experimental set up is shown schematically in Figure 1. It consists of a long channel of length L and height H which is packed with spheres of diameter D_p . This packed bed is fed with water (through a mechanism not shown, see original paper for more details) without any hydraulic head, so that the driving force for propagation is dominated by capillarity. The experiment consists of recording the movement of water as it propagates through an initially dry bed.

The geometric parameters of the experiment are the dimensions of the set up, (given as $L = 188.9mm$, $H = 12.7mm$, from Yendler, 1993), the sphere diameter, D_p for which values of 0.5, 0.75, 1.0, 1.5, 2.0 (all diameters in mm), and the porosity of the bed ϵ which has been reported to be in the range $\epsilon \approx 0.395 - 0.421$. Note that in any given experiment, beads of only a single size are used.

Defining the saturation θ , to be the fractional water content in the bed, ($\theta_{max} = \epsilon$), the experiment records δ which is some suitable value of θ , (say 0.99ϵ) as a function of time t . As is well known from the theory of two-phase immiscible capillary flow through porous

media (to be developed in the next section), $\delta \sim \sqrt{t}$.

In figure 2 we have redisplayed the results obtained by Yendler (1993). Figure 2a shows a plot of δ as a function of t for smaller sphere sizes, ($D_p = 0.5, 0.7, 1.0$) and 2b shows the same for $D_p = 1.5, 2.0$, mm. The interesting observation is that the rate of propagation is lower for the larger spheres. In the next section we will develop the equation governing the flow of liquid in unsaturated media and try to understand this peculiar behaviour.

2 Mathematical Formulation of Governing Equations

The equation governing the propagation of water through packed beds is the Richard's equation, given below (in dimensional form):

$$\frac{\partial \theta}{\partial t} = \nabla \cdot D \nabla \theta + \left(\frac{\rho g}{\mu} \right) \frac{dk}{d\theta} \frac{\partial \theta}{\partial y} \quad (1)$$

where $D = k \frac{d\psi}{d\theta}$. Here ψ is the capillary pressure and is a function of θ alone, k is the permeability of the medium. Hence the diffusion coefficient D , is also a function of θ making (1) a non-linear diffusion equation. The second term on the right hand side of (1) accounts for the effect of buoyancy. Richard's equation is based on the principle of continuity and D'Arcy's law. ¹

¹The continuity equation is $\frac{\partial \theta}{\partial t} + \nabla \cdot \mathbf{u} = 0$ and D'Arcy's law is given by $\mathbf{u} = - \left(\frac{k}{\mu} \right) \nabla \phi$, for a suitable pressure ϕ , which in our case can be decomposed into capillarity and hydraulic heads: $\phi = \psi(\theta) + \rho g y$. Combining the above three expressions yields (1) after some algebraic rearrangement.

According to Buckley-Leverett theory (see Bear 1972), the capillary head can be related to the surface tension and permeability of the medium as follows:

$$\psi = \frac{\sigma}{\sqrt{k}} J(\theta) \quad (2)$$

where σ is the surface tension and $J(\theta)$ is a function characteristic of the medium. The permeability k , is a function of both the nature of the porous media as well as the saturation θ . It is common to scale the permeability with respect to the characteristic grain size of the medium, (in our case, D_p) and a relative permeability to account for differences in saturation as,

$$\sqrt{k} = D_p G(\theta) \quad (3)$$

where $G(\theta)$ is the relative permeability. We note that both $G(\theta)$ and $J(\theta)$ are $O(1)$.

2.1 Non-dimensionalization

Choosing the characteristic length scale as H , the height of the apparatus, and $\frac{H^2 \mu}{\sigma D_p}$ as the characteristic time scale, (1) can be cast as:

$$\frac{\partial \theta}{\partial \tau} = \nabla \cdot G J' \nabla \theta + 2 G G' B_o \frac{\partial \theta}{\partial Y} \quad (4)$$

where τ is the rescaled time, and X, Y are the rescaled coordinates. The dimensionless group, $B_o = \frac{\rho g H D_p}{\sigma}$ is the Bond number and gives the relative importance of gravity and surface tension (capillarity). We note that D has the scale $\frac{\sigma D_p}{\mu}$, and thus the diffusivity scales linearly with D_p .

2.2 Flow with $Bo \rightarrow 0$

Setting $\mathcal{D} = G(\theta)J'(\theta)$ in (4) we obtain in the limit $Bo \rightarrow 0$

$$\frac{\partial \theta}{\partial \tau} = \nabla \cdot \mathcal{D} \nabla \theta \quad (5)$$

Seeking a one dimensional solution to (5), we write it as:

$$\frac{\partial \theta}{\partial \tau} = \frac{\partial}{\partial X} \mathcal{D} \frac{\partial \theta}{\partial X} \quad (6)$$

with initial and boundary conditions given by

$$\theta = 0 \quad \text{for } X > 0, \quad \tau = 0$$

$$\theta = \epsilon \quad \text{for } X = 0, \quad \tau > 0$$

Equation (5) with associated initial and boundary conditions admits a similarity solution in the similarity variable, $\eta = \frac{X}{\sqrt{\tau}}$ and

$$\frac{d}{d\eta} \mathcal{D} \frac{df}{d\eta} + \frac{\eta}{2} \frac{df}{d\eta} = 0 \quad (7)$$

where $f(\eta) = \theta(X, \tau)$. Solutions to this ODE can be obtained after making suitable assumptions for the functional dependence of $\mathcal{D} = \mathcal{D}(\theta)$. If it is assumed that \mathcal{D} is a constant, then

D_p, mm	m	$D = m^2$	$\frac{D}{D_p}$
0.46	1.194	1.425	3.097
0.75	1.533	2.350	3.130
1.00	1.493	2.229	2.229
1.50	0.723	0.273	0.182
2.00	0.100	0.010	0.005

Table 1: This table shows the effective diffusivity, D and examines the validity of its scaling with respect to D_p .

the solution has the form of the familiar complimentary error function. For $\mathcal{D} = \mathcal{D}(\theta)$, the equation becomes non-linear and generally needs to be solved numerically. This has been done by Phillip (1955), which can be consulted for more details. The results in Phillip (1955) show that the basic structure of the solutions remains the same as for linear diffusion, the exact profile being a strong function of the diffusion coefficient. Hence the locus of points for $\delta_{\theta=0.99}$ behaves as $\sim \sqrt{\mathcal{D}(\theta)\tau}$ as has been observed in Figure 2(a,b), where the propagation rate is shown to scale as \sqrt{t}^2 . Yendler et al (1993) also calculate the effective diffusivity, \mathcal{D} by fitting a line $l = m\sqrt{t} + b$ to the data of figure 2. Their results are given in table (1) where $D = m^2$, is the effective (dimensional) diffusivity.

The last column of the table examines the scaling of the effective diffusivity D with respect to D_p , the grain size and surprisingly, the relationship does not hold for $D_p > 0.75$. The only assumption in equation (1) is is D'Arcy's law which assumes that the Reynolds number

²Yendler et al have presented their results for unscaled (dimensional time)

D_p, mm	$U (cm/min)$	Re_{D_p}
0.50	33.33	2.75
0.75	20.00	2.50
1.50	6.00	1.50
2.00	0.26	0.53

Table 2: This table shows the Reynold's number, Re_{D_p} , for the range of D_p considered.

of the flow is low. There is considerable experimental data (see for example Bird, Stewart, Lightfoot , 1960, page 198) which suggests that D'Arcy's law is valid for a pore Reynolds number, $Re_{D_p} < 10$.

Using data available from the experiments, we have estimated $Re_{D_p} = \frac{UD_p}{\nu}$, using $\nu = 10^{-6} m^2 s^{-1}$ and found the value to be less than 3 for all the pore sizes considered from 0.50 to 2.0. This is shown in table (2) where the velocity (as obtained from experiments) and the calculated Reynolds number are given

The capillary number, $Ca = \frac{UD_p}{\sigma}$, has been found to be of the order of 10^{-4} (using $\sigma = 70 \times 10^{-3} Nm^{-1}$, and a reference velocity scale). Thus the capillary forces are dominant with respect to at the pore scales. Hence we conclude that (1) should correctly predict the behaviour of the fluid in the given range of sphere diameters.

D_p, mm	Bo
0.50	1.57
0.75	2.35
1.00	3.14
1.50	4.71
2.00	6.28

Table 3: This table shows the Bond number, Bo for the range of D_p considered.

2.3 Effect of Bond number, Bo

Horizontal propagation of water through a bed of packed spheres was studied with the implicit assumption that gravity is not an important factor, and hence the model could be used to study similar situations in microgravity environments. This assumption now needs to be re-evaluated in light of the discrepancy observed between one-dimensional theory as developed in the previous section and the experimental results.

Using $\rho = 10^3$, $g = 10$, $\sigma = 70 \times 10^{-3}$, and $H = 12 \times 10^{-3}$, (all in SI units) the Bond number is calculated and shown in table (3). We note that $Bo > 2.5$ for the larger spheres and hence gravity is significant in (1) and cannot be ignored.

3 Conclusion and suggestion for further work

We have shown that the Bond number is significantly large (greater than 1) for the larger sphere diameters under consideration and hence gravity plays a significant role in the outcome of the experiment. This could be responsible for the diminished rate of propagation that has been observed. ³

It may be possible to overcome this difficulty, simply by controlling the Bond number. Since we may desire to maintain the grain size and the size of the apparatus at current values, the only parameters left are the liquid density and surface tension. Hence it may be possible to conduct the experiment successfully by a suitable choice of liquid, with higher surface tension and lower density. Table 3 suggests that a factor of 6 – 10 reduction in Bond number would be sufficient.

References

BEAR, J. (1972) Dynamics of Fluids in Porous Media. Dover Publications.

³Towards the end of this study, the author learned that the effect of gravity was so strong for the larger sized spheres that the height of the liquid column in the apparatus was no more than the capillary rise, showing that there was a clear balance of forces between capillarity and gravity. This also explains the diminished rate of propagation since part of the capillary suction is utilized in overcoming the gravitational head when siphoning water from the reservoir into the packed bed. Hence the current design of the experiment no longer meets the objective of using horizontal propagation to model propagation in low gravity environments.

BIRD, R.B , STEWART, W. E. & LIGHTFOOT, E. N. (1960) Transport Phenomena. John Wiley and Sons.

PHILLIP, J.R. (1955) Numerical Solution of Equations of Diffusion type with diffusivity concentration dependent. Transactions of Faraday Society, 51, pps. 885-892.

YENDLER, B & WEBBON, B. (1993) Capillary movement of liquid in Granular beds. SAE Tech. Paper No. 932164, 23rd Conference on Environmental Systems.

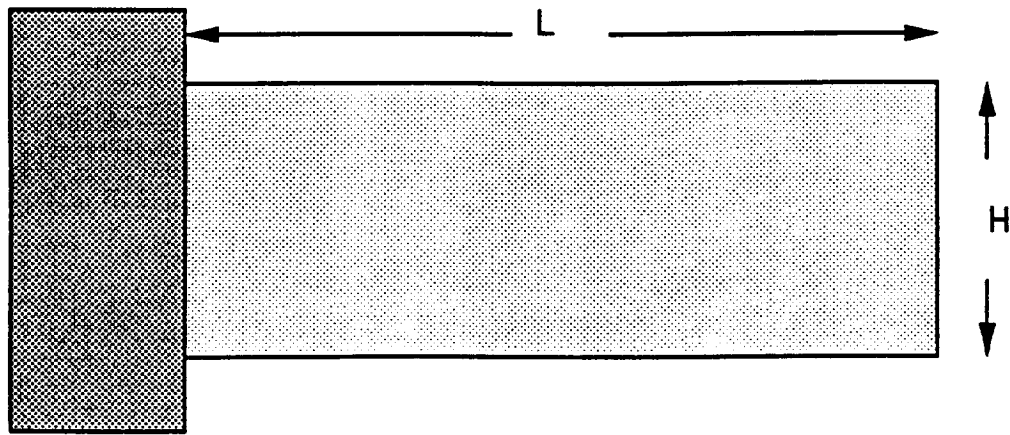


Figure 1: Schematic Layout of the Experiment.

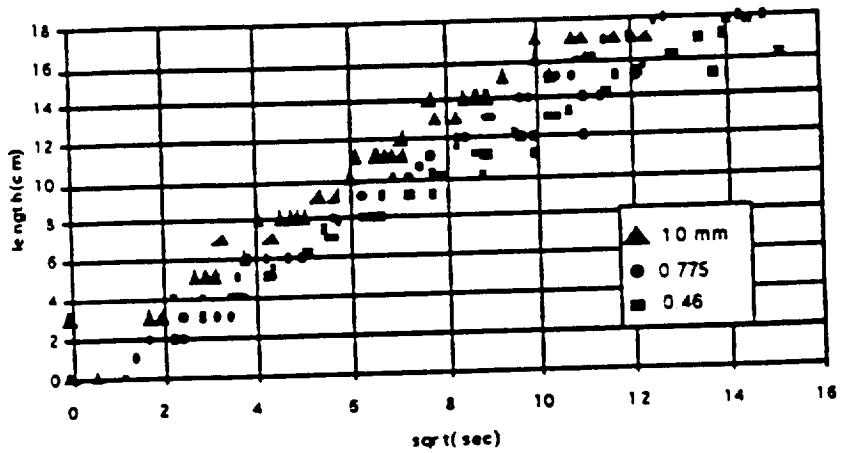


Fig. 2a

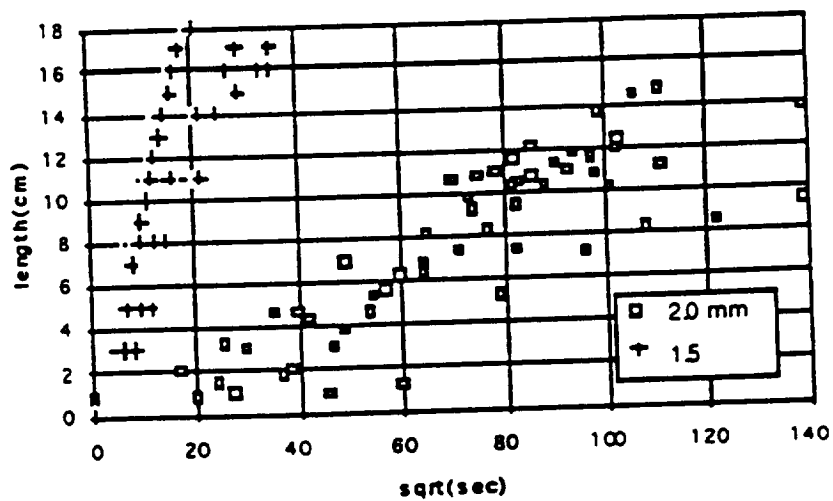


Fig. 2b

Figure 2: Experimental results obtained by Yendler (1993).